

Ultrasonic torsional guided wave sensor for flow front monitoring inside molds

Karthik Visvanathan and Krishnan Balasubramaniam

Citation: [Review of Scientific Instruments](#) **78**, 015110 (2007); doi: 10.1063/1.2432258

View online: <http://dx.doi.org/10.1063/1.2432258>

View Table of Contents: <http://scitation.aip.org/content/aip/journal/rsi/78/1?ver=pdfcov>

Published by the [AIP Publishing](#)

Articles you may be interested in

[ON THE OPTIMIZATION OF TEMPERATURE COMPENSATION FOR GUIDED WAVE STRUCTURAL HEALTH MONITORING](#)

AIP Conf. Proc. **1211**, 1860 (2010); 10.1063/1.3362320

[Separated two-phase flow regime parameter measurement by a high speed ultrasonic pulse-echo system](#)

Rev. Sci. Instrum. **78**, 114901 (2007); 10.1063/1.2804117

[Stability analysis of injection molding flows](#)

J. Rheol. **48**, 765 (2004); 10.1122/1.1753276

[Experimental And Numerical Study Of The Melt Behavior During The Injection Molding Process](#)

AIP Conf. Proc. **712**, 157 (2004); 10.1063/1.1766516

[Structural Health Monitoring of Anisotropic Layered Composite Plates Using Guided Ultrasonic Lamb Wave Data](#)

AIP Conf. Proc. **700**, 1460 (2004); 10.1063/1.1711787

Nor-Cal Products



Manufacturers of High Vacuum
Components Since 1962

- Chambers
- Motion Transfer
- Flanges & Fittings
- Viewports
- Foreline Traps
- Feedthroughs
- Valves



www.n-c.com
800-824-4166

Ultrasonic torsional guided wave sensor for flow front monitoring inside molds

Karthik Visvanathan and Krishnan Balasubramaniam^{a)}

Centre for Nondestructive Evaluation, Indian Institute of Technology Madras, Chennai 600 036, India and
Department of Mechanical Engineering, Indian Institute of Technology Madras, Chennai 600 036, India

(Received 5 October 2006; accepted 18 December 2006; published online 29 January 2007)

Measuring the extent of flow of viscous fluids inside opaque molds has been a very important parameter in determining the quality of products in the manufacturing process such as injection molding and resin transfer molding. Hence, in this article, an ultrasonic torsional guided wave sensor has been discussed for monitoring the movement of flow front during filling of resins in opaque molds. A pair of piezoelectric normal shear transducers were used for generating and receiving the fundamental ultrasonic torsional guided wave mode in thin copper wires. The torsional mode was excited at one end of the wire, while the flowing viscous fluid progressively wet the other free end of the wire. The time of flight of the transient reflections of this fundamental mode from the air-fluid interface, where the wire enters the resin, was used to measure the position of the fluid flow front. Experiments were conducted on four fluids with different viscosity values. Two postprocessing algorithms were developed for enhancing the transient reflected signal and for suppressing the unwanted stationary signals. The algorithms were tested for cases where the reflected signals showed a poor signal to noise ratio. © 2007 American Institute of Physics.

[DOI: 10.1063/1.2432258]

INTRODUCTION

Improper filling and undercuring of viscous fluids such as polymeric resin have been a concern in many industries such as polymers, composites, etc., resulting in increased manufacturing costs and poor performance of the fabricated structures. Different methods have been investigated to determine proper curing of the resin especially using guided waves in different waveguides. Papadakis¹ in 1974 proposed two methods for determining the change in material properties during the curing of the epoxy resin. The first method was based on the measurement of attenuation of both longitudinal and torsional modes in circular rods. The second one was based on measuring the reflection of the waves at the interface where the waveguide enters the epoxy resin. After that, Harrold and Sanjana² used guided waves in rod for monitoring the cure of composites. A U-bent wire was used by Li *et al.*³ in a through transmission arrangement for monitoring the cure of epoxy resin in composite column wraps for highway applications. Their work was also based on measuring the change in guided wave attenuation as the resin cures. Further, Vogt *et al.*⁴ provided the measurement techniques, as proposed by Papadakis, a theoretical foundation based on guided wave theory and numerical modeling. Further, Fomitchov *et al.* discussed the use of the laser ultrasonic array system for monitoring the cure in Ref. 5.

However, very limited work has been done on methods to ensure complete filling of the molds with resin. Laser based flow sensors such as laser Doppler velocimeter and

laser time-of-flight velocimeter have been in use for a very long time. However, these methods are useful only in transparent molds. Secondly, the commercial ultrasonic flow meters generally work on two principles. The first type, called transit time ultrasonic flow meter, operates by comparing the time for a signal to travel with the flow (downstream) with the time for a signal to travel against the flow. While the other, called Doppler ultrasonic flow meter, operates by sensing the frequency shifts of the signal reflected from moving particles, bubbles, or density differences, thereby producing a linear signal proportional to the flow of the fluid. Further details on these sensors can be found from Refs. 6–10. But both the above sensors are incapable of measuring the flow front, thereby rendering them incapable of determining the percentage of the volume of mold filled with resin. Kim *et al.*¹¹ developed a torsional waveguide of diamond cross section to sense online and in real time the characteristics of the liquid as well as the liquid level. Since thin wires are preferred (in order to reduce the inhomogeneity in the final product due to the presence of wire), making diamond cross sections in these wires would prove very expensive.

Furthermore, a novel technique for combining a conventional Rhodes flow meter with advanced technology of fiber optic sensor was proposed in Ref. 12. A novel fiber optic real-time sensor system that can sense resin at various locations on a single fiber using long-period gratings and a polychromatic source was discussed in Ref. 13. In addition to it, a soft sensor based on a recurrent neural network was developed to predict the melt-flow-length during injection mold filling in Ref. 14. This sensor is trained using the experimental data obtained from a set of purposely designed molds with basic feature geometry. Next, the feasibility of using

^{a)} Author to whom correspondence should be addressed; electronic mail: balas@iitm.ac.in

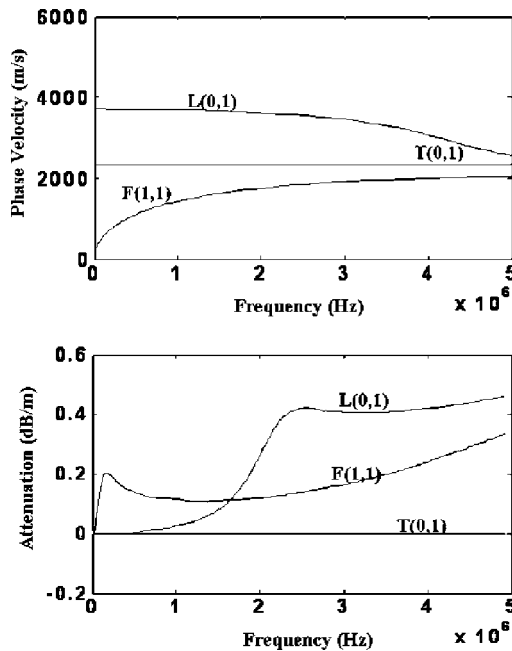


FIG. 1. (a) Phase velocity vs frequency and (b) attenuation vs frequency curves for wave modes in copper wire (density=8900 kg/m³, shear wave velocity=2330 m/s, and longitudinal velocity=4660 m/s) of radius 0.25 mm in air plotted using DISPERSE.

optical fibers with long-period gratings (LPGs) as sensors for monitoring flow in the liquid composite molding (LCM) process was investigated in Ref. 15. The LPGs are sensitive to changes in the refractive index and register a strong signal change when covered with resin.

Stoven *et al.*¹⁶ proposed an idea for monitoring the flow front propagation of resin utilizing ultrasound transmission. In this, an acoustic pulse is transmitted, moving perpendicularly through stacks of fibers, and is received by an ultrasonic transducer at the other end. Infiltrating the fibers with a liquid in thickness direction would result in change in the speed of propagation. This was measured to determine whether the flow has taken place at that point or not. However, this technique requires considerable compactness between the fibers in the transverse direction for the wave to propagate through them. Moreover, it also requires the signals to be taken at various locations for locating the exact flow front.

In this article, we present a cost effective method for monitoring the flow front of resin in injection molding and resin transfer molding (RTM) industries. Besides, it can also be used in industries where flow front measurement is required for fluids of viscosities greater than 50 cP. Moreover, the same sensor can be used as a leak/level indicator.

THEORY

The main motivation for the work presented here is to develop a low cost but accurate sensor, which overcomes the limitations of the existing sensors for monitoring proper filling of the molds in real time. The sensor discussed here generates guided waves in thin wire waveguides. Because of the change in surface impedance at the point where the wire enters the embedding fluid, the guided wave will get reflected and scattered through mode conversions. The time of

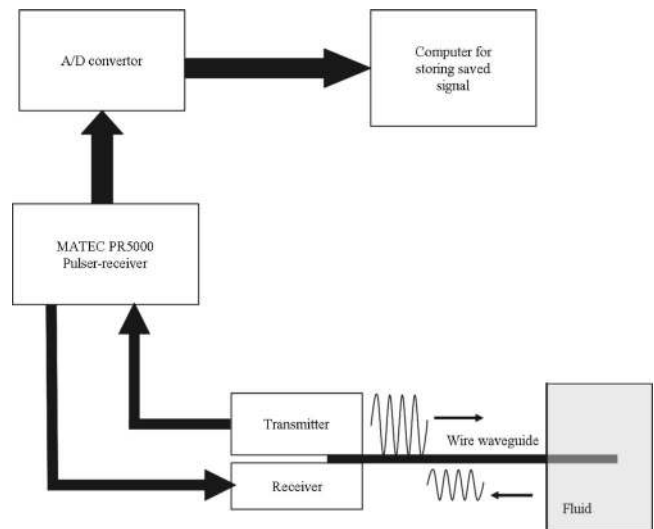


FIG. 2. Schematic representation of the experimental setup used in the experiment.

flight of the reflected wave depends on the distance of the flow front from the transducer. As the flow front moves along the waveguide, the reflected signal also advances in time. Thus, it is capable of providing information about the extent to which mold has been filled with resin. Vogt *et al.*¹⁷ discussed a more detailed explanation and numerical model describing the scattering of the guided wave in partly embedded cylindrical structures. The distance of the flow front from the transducer can be calculated from

$$t = \frac{2^*d}{v_s}, \quad (1)$$

where t is the time of flight of the reflected wave, v_s is the velocity of the torsional mode in the waveguide, and d is the distance of the transducer from the air-fluid interface. The velocity of the guided wave can be computed from the dispersion curves shown in Fig. 1, plotted using DISPERSE.¹⁸

In a free waveguide, i.e., one surrounded with air, the attenuation occurs only due to the losses in the waveguide material. Thus, less attenuating materials such as metals were used for transmitting the guided waves. This provides an advantage of having longer waveguides enabling the placement of transducers at a distance from the mold.

Three different families of modes can be generated in cylindrical rods, namely, longitudinal $L(0,n)$, torsional $T(0,n)$, and flexural $F(m,n)$, where m and n represents the mode symmetry and mode order, respectively, as per the Silk and Bainton notation.¹⁹ Each family of modes itself comprises infinite number of modes. The longitudinal mode has a displacement in both radial and axial directions, while the torsional mode has a displacement only in the circumferential direction. On the other hand, flexural modes have displacements on all the three directions. The presence of a large number of waveguide modes complicates the data analysis, and hence is not preferred. Moreover, in the case of thin wires these modes cannot be separated by methods used in pipe testing, where an array of transducers that are circumferentially placed are used to separate modes, based on mode shapes.²⁰ Hence, it is preferred to work with the frequencies

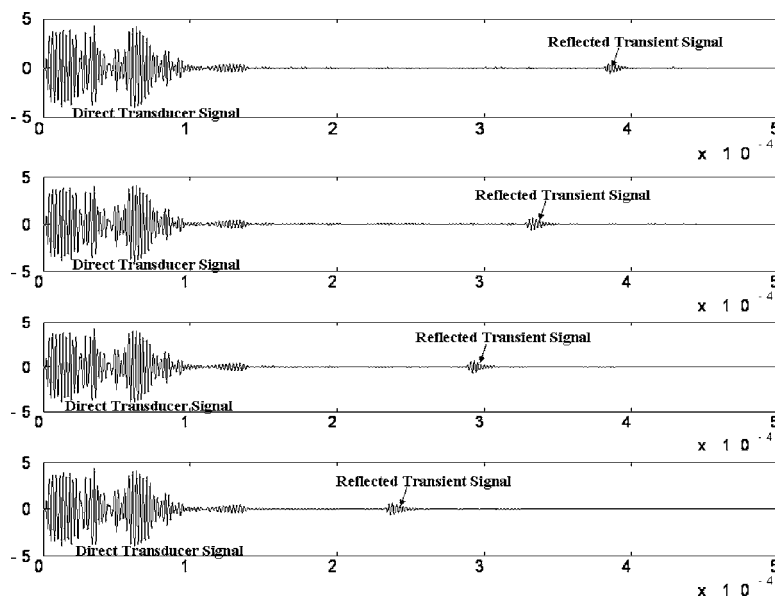


FIG. 3. A-scan signals collected at various time instances for reflection from the interface of viscosity standard N4000.

where only fundamental modes are present. Secondly, for the application stated, the transducer has to be kept far from the actual location of the measurement and must provide a sufficiently strong signal from the air-fluid interface. Since, the fundamental torsional mode, $T(0, 1)$, has the least attenuation and dispersion in copper wires (see Fig. 1), this mode was selected. Moreover, the torsional wave modes are expected to be more sensitive to rheological changes in the fluid and provide a relatively higher reflected signal at the air-fluid interface when compared to the longitudinal and flexural modes.

EXPERIMENTAL SETUP

A pair of 0.5 MHz piezoelectric shear transducers [Panametrics V151 Videoscan Y-cut normal lead zirconic titanate (PZT) shear wave probe] placed on either side of the waveguide were used for generating torsional modes in the wire waveguide. One of the transducers act as a transmitter, while the other acts as a receiver. With the help of a suitably designed probe holder the transducer's vibration direction was ensured to be perpendicular to the axis of the waveguide, in order to predominantly generate torsional modes in the waveguide. A three-cycle Hanning window tone burst signal was used to excite the transducer. The frequency of the shear transducers was chosen to be 0.5 MHz so that only the fundamental modes are generated in the rod, as shown by the dispersion curve in Fig. 1. Restricting the generation of the higher order modes greatly helps in reducing the complexity in postprocessing algorithm.

Next, a 0.5 mm diameter copper wire (density = 8900 kg/m^3 , shear wave velocity = 2330 m/s , and longitudinal velocity = 4660 m/s) is used as the waveguide for transmitting the torsional mode. The strength of the reflected signal from the air-fluid interface depends on the viscosity, density, waveguide diameter, and frequency of operation.²¹ The reflection coefficient is proportional to viscosity and density and inversely proportional to the diameter and fre-

quency product. Also, the attenuation of the wave in the material depends on the material, the length, and the frequency of operation. Here, the attenuation contribution due to the leakage of the wave into fluid is not relevant, since only the reflected signal is considered. For a low viscous fluid a shorter wire has to be used, as the energy reflected from the interface is quite small. However, the wire must be long enough so that the reflected wave from the interface does not merge with the initial directly transmitted signal between the transmitter and receiver transducers. Based on studies conducted, it was found that if the viscosity of the fluid is above 700 cP, then the length of the wire could be up to 700 mm. During the experiments, wires of lengths varying from 500 to 1200 mm were used. Additionally, the end of the wire must be made as planar as possible so that conversions into other modes, especially into the fundamental flexural mode, can be avoided. The torsional wave is generated in both directions, one towards the viscous fluid and the other in the opposite direction. If this other end is a free end, the reflected guided waves from this end overlap with the useful reflected signal coming from the fluid interface. In order to avoid this interference, the other free end of the wire was covered with a material having high damping capabilities. For the experiment discussed here, an adhesive tape was used as the damping material.

As an alternative, magnetostrictive methods can also be

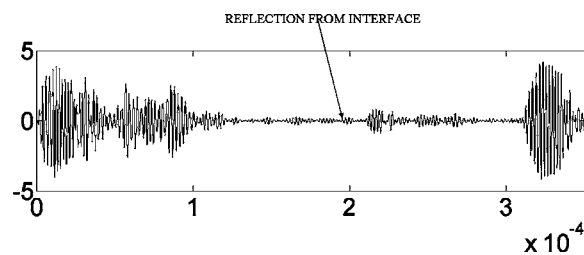


FIG. 4. A-scan signal of the reflection from the water-glycerol mixture interface.

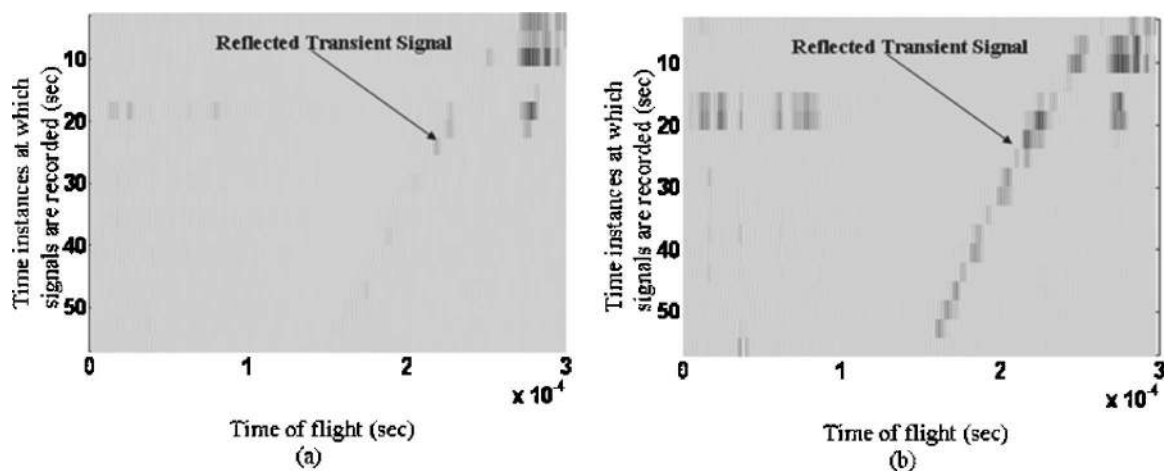


FIG. 5. Processed B-scan images for data collected for vinyl ester resin. (a) Processed signal obtained by iteratively subtracting signal at time instance $i - 1$ from the signal at i . (b) Processed signal obtained by iteratively subtracting the mean of the signal at time instances $i - 1$ and $i + 1$ from the signal at time instance i .

used for exciting torsional waves in rods. First, the waveguide is permanently magnetized in the circumferential direction and then placed in a coil carrying alternating current (Wiederman effect).²² The inverse magnetostrictive effect provides an opportunity for using the same coil as the receiver. However, for the experiment presented here the piezoelectric way of exciting torsional modes has been used.

A matec PR5000 pulser-receiver is used for exciting the transmitter transducer and for receiving the signal from the receiver transducer. For the experiments performed three-cycle pulses were generated using the pulser. The received analog signal was digitized using a National Instruments PCI 5102 20 MHz analog to digital converter for converting the analog signal received into a digital form, and the signals are stored and processed in a computer. A LABVIEW program capable of collecting and storing the signal at a fixed interval time has also been developed. A schematic diagram of the experimental setup is shown in Fig. 2.

POSTPROCESSING

Typical A-scan signals at various time instances obtained using NIST traceable viscosity standard Cannon N4000 (viscosity=10 400 cP and density=879 kg/m³) are shown in Fig. 3. Here the reflected signal from the interface is very clearly observed during the pour of the fluid. However, with the decrease in the viscosity of the fluid the amount of energy reflected from the interface decreases. This results in the useful signal being masked by the noise and the reflections from unavoidable kinks in the thin waveguide. A typical signal from the interface of the glycerol water mixture (viscosity=65 cP and density=1213 kg/m³) is shown in Fig. 4. The very weak nature of the reflected signal from the interface of low viscous fluids calls for the development of a postprocessing algorithm for enhancing the interface reflected signal and for suppressing the unwanted stationary signal.

Two different postprocessing algorithms were developed for enhancing the signal and are described below.

Method 1

The A-scan signals at different time instances are combined to form a B-scan image $S(i, j)$, where i represents each instant of data recording during mold filling and j represents the discrete time-of-flight data of the signal. The $S(i, j)$ matrix is plotted in the form of intensity plot, as a gray scale image. This method takes advantage of the fact that except for the signal reflected from the moving flow front, all the other signals including the ones from the kinks remain sta-

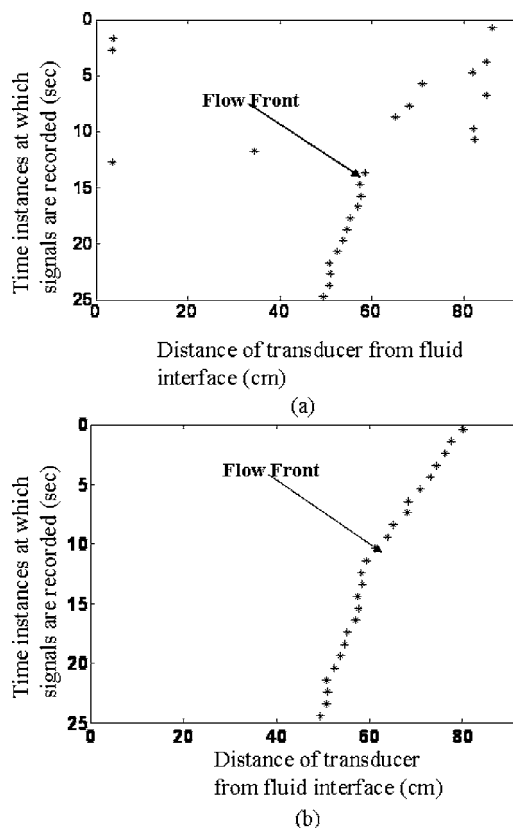


FIG. 6. (a) Flow front curve for glycerol without using the local maxima search method. (b) Flow front curve for glycerol after using the local maxima search method.

tionary (unchanged) during the filling process. Hence, an iterative process of subtracting the time signal at time instant $i-1$ from the signal at time instant i is performed on the signals collected by the data acquisition system as shown in.

$$S^1(i,j) = S(i,j) - S(i-1,j). \quad (2)$$

This results in suppressing the strong stationary signal to a certain extent without affecting the weakly moving reflected signal from the flow front. However, the stationary signals, as shown in Fig. 5(a) for vinyl ester resin, are not suppressed quite well by this method. This is because the amplitude of the stationary signals keeps changing due to the attenuation in the viscous fluid. Hence, in order to estimate the stationary signal better, the mean of the signals at time instant $i-1$ and at time instant $i+1$ is used as

$$S^2(i,j) = S(i,j) - \frac{S(i+1,j) + S(i-1,j)}{2}. \quad (3)$$

The result obtained from subtracting this mean from the signal at time instant i is shown in Fig. 5(b) for the case of the vinyl ester resin. However, one has to note that for the subtraction algorithm rate at which the signals are taken is a function of the rate at which the flow front moves. If the signals are taken too fast as compared to the flow rate, then on subtraction a significant part of the signal might get canceled. Hence in the general case n signals ($i-1, i-2, \dots, i-n$) are subtracted from the i th signals and are added together. Moreover, the removal of the initial transducer band

improves the output image quality of the algorithm. However, in the processing done here, subtraction of the previous time frame alone gives a good result.

Method 2

This method is based on filtering in frequency domain. First, a two-dimensional Fast Fourier transform (FFT) along the y direction of the B-scan image was obtained. The two-dimensional (2D)-FFT along the y direction indicates the frequency content of the change in the A-scan signal between two adjacent time instances. By using a high pass filter along the y direction, the stationary signals whose amplitudes slowly vary due to the attenuation can be suppressed. The high pass filter is achieved by multiplying a suitable filter mask with the 2D-FFT. Finally, a 2D inverse Fourier transform was employed to obtain the final processed B-scan image.

From the processed B-scan images, the flow front profile was extracted by first obtaining the time of flight of the maximum amplitude of the signal in each row (representing the reflected peak of the A scan at any time instance). Since, in some of the B scan, the signal to noise ratio was low, all of these maxima may not necessarily correspond to the peak of the reflected signal, as shown in Fig. 6(a). Hence, the median of the time-of-flight data of these maxima was taken as the seed. This ensures that the seed value used for the local search or the flow front profile is more robust. Let this value be $S(i,j)$. Using this seed as a starting point, the

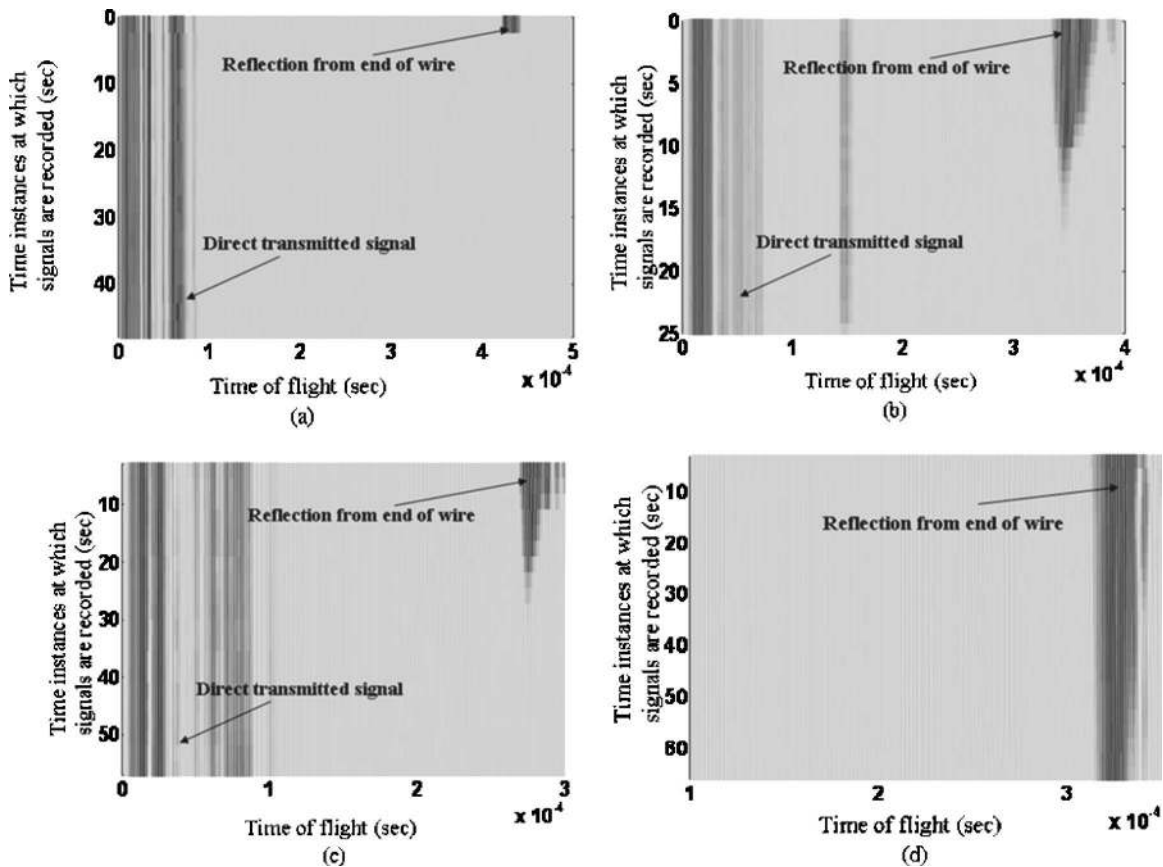


FIG. 7. Unprocessed B-scan images. (a) Cannon N4000, (b) glycerol, (c) vinyl ester resin, and (d) glycerol-water mixture.

TABLE I. Properties of viscous fluids used in experiments .

Sample No.	Name	Density (kg/m ³)	Viscosity (cP)
1	Viscosity standard N4000	879	10 400
2	Glycerol	1258	1440
3	vinyl ester resin	1030	275
4	Glycerol-water mixture	1213	65

maxima in the adjacent rows were obtained by confining the search only to the near vicinity of the previous found maxima, say, from $S(i-1, j-n)$ to $S(i-1, j+n)$, where n is between 100 and 150. Let $S(i-1, k)$ be the local maxima in the $i-1$ th row. Now this is taken as the j value for row $i-2$. This is carried out until the value of i becomes 1. Similarly, we carry out the same calculation for the rows $i+1$ to N , where N is the number of rows in the B-scan image. Finally, these maximum points in each row were joined in order to visualize the flow front profile, as shown in Fig. 6(b). From the flow front profile, which is essentially the time-of-flight data, the distance of the flow front from the transducer was calculated using Eq. (1), using the velocity of the fundamental torsional mode in the waveguide.

EXPERIMENTAL RESULTS AND DISCUSSION

The experiment was conducted on four different fluids having different viscosities and densities. The properties of

the four fluids are indicated in Table I. The quality of the A-scan signals collected was found to depend on the orientation of the shear transducers with respect to the axis of the waveguide. The direction of the vibration of the shear transducers have to coincide with the circumferential direction so that the generation of other modes could be minimized.

The raw B-scan images for the four cases are shown in Figs. 7(a)–7(d). The y axis of these figures indicates the time instances at which the signals were collected. Thus, each row represents a signal taken at a particular time instant. For the viscosity standard Cannon N4000, even though the reflected signal from the interface is strong enough, the presence of the strong reflection from the immersed end of the wire during initial time instants suppresses the reflected signal in the B-scan image. However, due to the reduced viscosity of the other fluids, one can clearly see the difficulty in identifying the reflected signal in the images. The processed B-scan images from the two postprocessing algorithm are shown in Figs. 8(a)–8(d) and Figs. 9(a)–9(d), respectively. The effectiveness of the algorithm is clearly seen especially for the glycerol-water mixture, where the reflected signal was completely masked by the noise and reflection from the bends and other modes generated in the rod. All the algorithms were found to agree well with one another. Finally, the flow front curves for the four cases are shown in Figs. 10(a)–10(d). Even though both the algorithms are found to produce equally good results, the simplicity of the first algorithm helps in providing a way for simultaneous real-time monitoring of the flow front. The sensor with the help of postprocessing algorithm, described in the previous section,

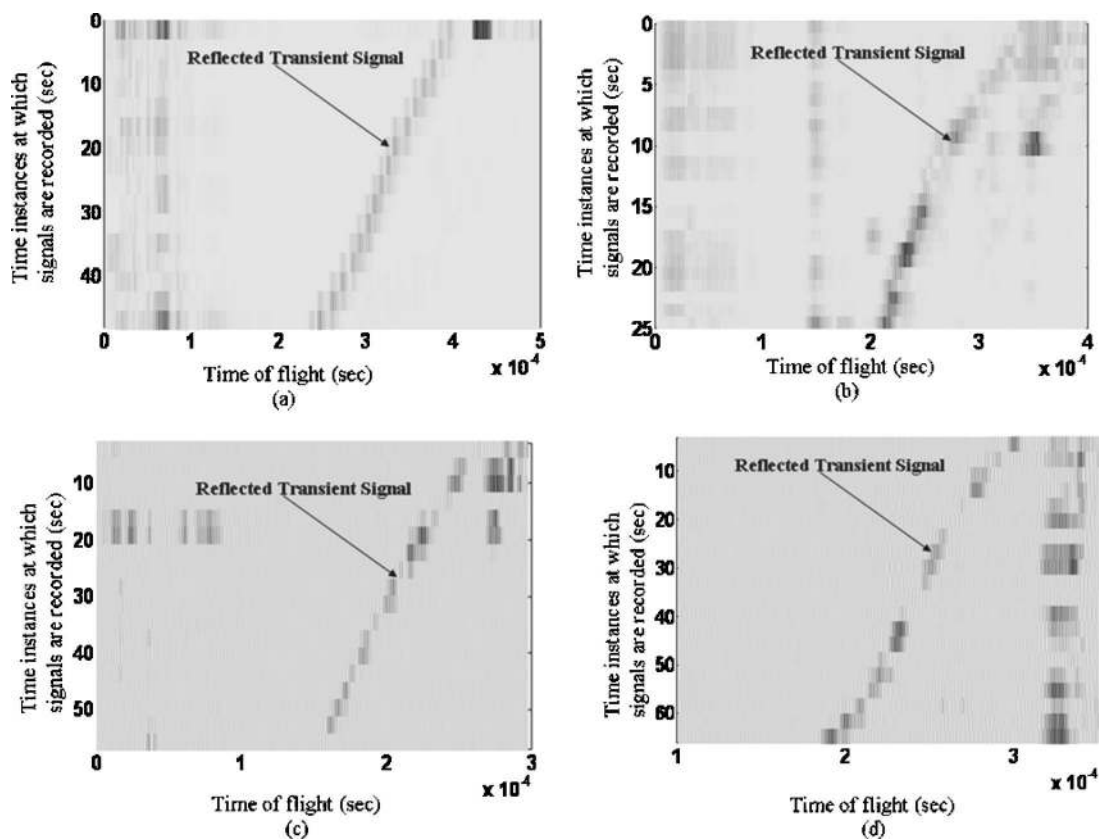


FIG. 8. Processed images using algorithm 1. (a) Cannon N4000, (b) glycerol, (c) vinyl ester resin, and (d) glycerol-water mixture.

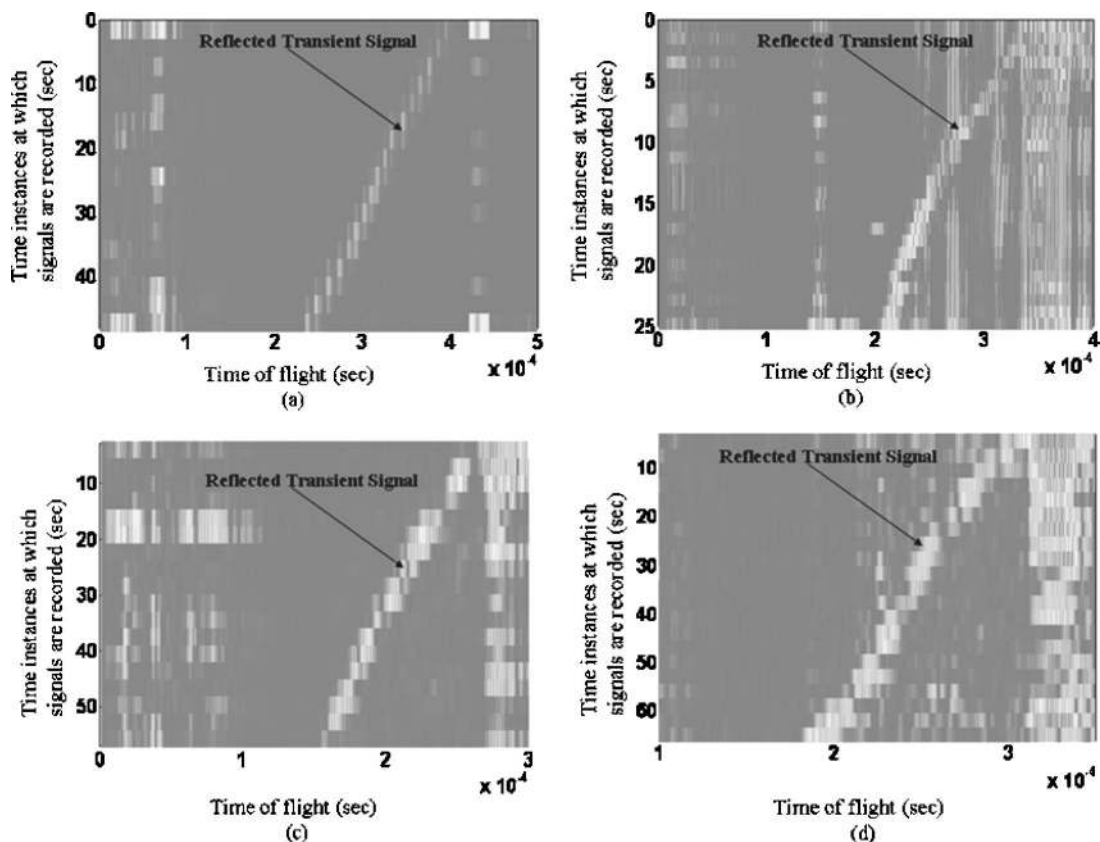


FIG. 9. Processed images using algorithm 2. (a) Cannon N4000, (b) glycerol, (c) vinyl ester resin, and (d) glycerol-water mixture.

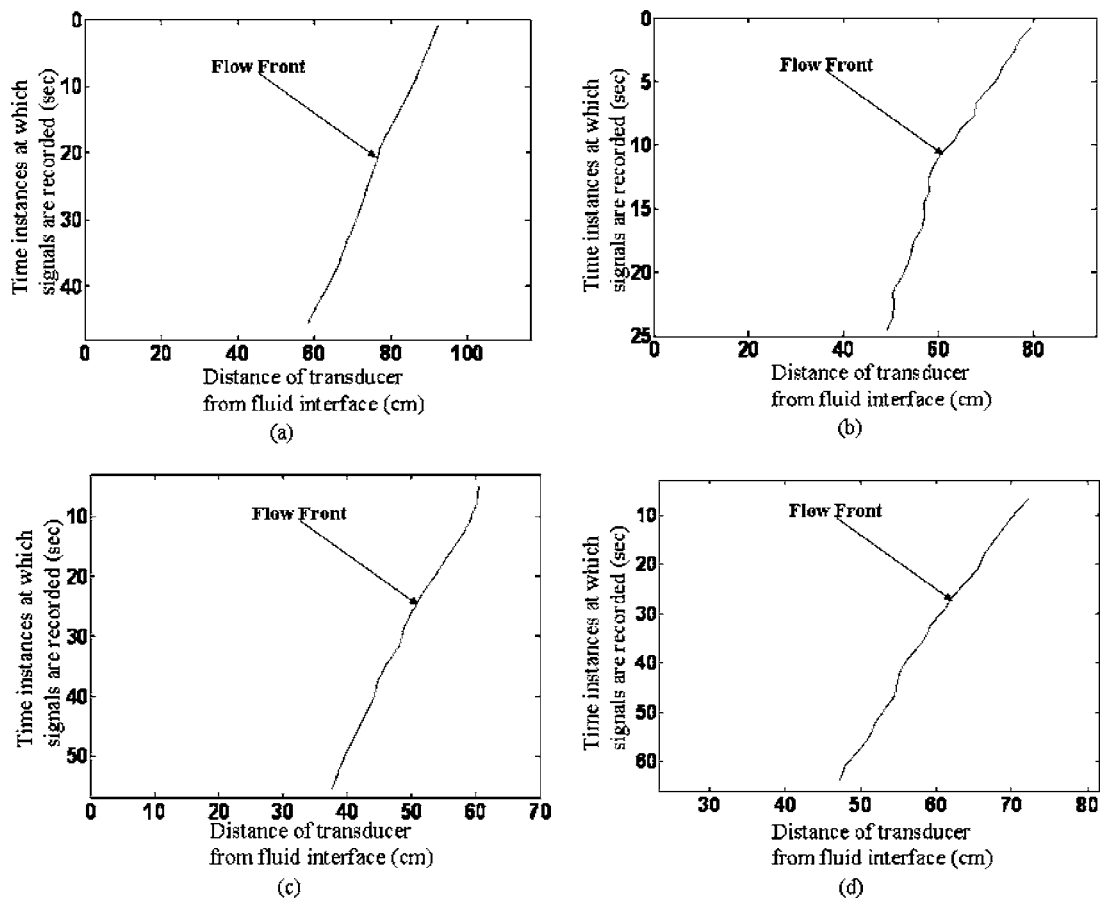


FIG. 10. Flow front curve. (a) Cannon N4000, (b) glycerol, (c) vinyl ester resin, and (d) glycerol-water mixture.

was found to work well for fluids with viscosity as low as 65 cP. In addition, suppressing the initial transducer band through time gating was found to improve the quality of the final image.

DISCUSSION

A waveguide sensor for monitoring the flow front of fluids inside a mold has been developed and tested on different fluids. The sensor works by measuring the time of flight of a transient fundamental torsional mode that is supported in a very thin wire and is reflected from the air-fluid interface (at the point of entry of the wire into the fluid), while the fluid front approaches a stationary transducer. For high viscous fluids, the transient reflected signals were very strong compared to other signals, such as reflections/scattering from the wire end and from small unavoidable “kinks” in the wire. As the viscosity of the fluid decreases, the strength of the reflected signals reduces as compared to the other reflected/scattered signals. Hence, two different postprocessing algorithms (one based on time domain analysis and one based on frequency domain analysis) were developed for enhancing the weak transient reflected signal from the interface and for suppressing the other stationary reflections and noises. Both methods showed an improvement in enhancing the contrast of the interface reflected signal. Method 1, which uses time domain processing, was found to be better, since the frequency domain approach had residuals from stationary signals. However, the contrast of the moving signal to the background noise in image was found to be better in case of method 2. The postprocessed B-scan images were then used to plot the flow front profiles for different fluids. While this sensor has been shown to work in certain fluids, this approach can be used in many other applications such as level sensing and high temperature process monitoring and may be used for a wide range of fluids. However, this method was found to be relatively insensitive to fluids with viscosity less than 65 cP.

Another added advantage of the sensor is that the same sensor can be used for monitoring the cure of the resins as

discussed in Ref. 21. Usage of thin wire reduces the adverse effect of foreign materials present in the resin products.

ACKNOWLEDGMENTS

The authors would like to thank the Research and Development Engineers (Est.), Dighe, Pune, India for their kind support of this project. They also thank the Composites Technology Centre, IIT Madras for carrying out the measurements of viscosity of the fluids using the rotating viscometer.

- ¹E. P. Papadakis, *J. Appl. Phys.* **45**, 1218 (1974).
- ²R. T. Harrold and Z. N. Sanjana, *Polym. Eng. Sci.* **26**, 367 (1986).
- ³Y. Li, G. J. Posakony, and S. M. Menon, Proc. 43rd International SAMPE Symposium, Anaheim, CA, 1998 (unpublished), pp. 937–948.
- ⁴T. Vogt, M. Lowe, and P. Cawley, *J. Acoust. Soc. Am.* **114**, 1303 (2003).
- ⁵P. F. Fomitchov, Y. Kim, A. Kromine, and S. Krishnaswamy, *J. Compos. Mater.* **36**, 1889 (2002).
- ⁶R. C. Asher, *Ultrasonic Sensors* (Institute of Physics Bristol, 1998).
- ⁷A. E. Brown, *Ultrasonic Flowmeters Flow Measurement: Practical Guides for Measurement and Control* (Instrument Society of America, Research Triangle Park, NC, 1991), pp. 415–442.
- ⁸K. I. Jespersen, National Engineering Laboratory Internal Report No. 552, 1973 (unpublished).
- ⁹L. C. Lynnworth, *Ultrasonic Measurements for Process Control* (Academic, New York, 1989).
- ¹⁰L. C. Lynnworth, *Ultrasonic Flowmeters Physical Acoustics: Principles and Methods* (Academic, New York, 1979), pp. 407–525.
- ¹¹J. O. Kim *et al.*, *IEEE Trans. Ultrason. Ferroelectr. Freq. Control* **40**, 563 (1993).
- ¹²A. Meng, S. Huang, W. Chen, and F. Luo, *Proc. SPIE* **2839**, 409 (1996).
- ¹³J. P. Dunkers, J. L. Lenhart, S. R. Kueh, J. H. Van Zanten, S. G. Advani, and R. S. Parnas, *Opt. Lasers Eng.* **35**, 91 (2001).
- ¹⁴Chen Xi, G. Furong, and C. Guohua, *Mater. Sci. Eng., A* **384**, 245 (2004).
- ¹⁵S. R. M. Kueh *et al.*, *Proc. SPIE* **3993**, 240 (2000).
- ¹⁶T. Stoven, F. Weyrauch, P. Mitschang, and M. Neitzel, *Composites, Part A* **34A**, 475 (2003).
- ¹⁷T. Vogt, M. J. S. Lowe, and P. Cawley, *J. Acoust. Soc. Am.* **113**, 1258 (2003).
- ¹⁸B. N. Pavlakovic, M. J. S. Lowe, D. N. Alleyne, and P. Cawley, *Rev. Prog. Quant. Nondestr. Eval.* **16**, 185 (1997).
- ¹⁹M. G. Silk and K. F. Bainton, *Ultrasonics* **17**, 11 (1979).
- ²⁰D. N. Alleyne, B. Pavlakovic, M. J. S. Lowe, and P. Cawley, *Insight* **43**, 93 (2001).
- ²¹T. Vogt, Ph.D thesis, Imperial College of Science, Technology and Medicine, London, UK, 2002.
- ²²N. S. Tzannes, *IEEE Trans. Sonics Ultrason.* **SU-13**, 33 (1966).